Quench dynamics of the topological quantum phase transition in the Wen-plaquette model

Long Zhang, Su-Peng Kou, and Youjin Deng

Phys. Rev. A **83**, 062113 — Published 17 June 2011

DOI: 10.1103/PhysRevA.83.062113

Quench dynamics of the topological quantum phase transition in the Wen-plaquette model

Long Zhang,[1] Su-Peng Kou,[2,*] and Youjin Deng[1]

[1]*Hefei National Laboratory for Physical Sciences at Microscale and Department of Modern Physics, University of Science and Technology of China, Hefei, Anhui 230026, China*
[2]*Department of Physics, Beijing Normal University, Beijing 100875, China*

We study the quench dynamics of the topological quantum phase transition in the two-dimensional transverse Wen-plaquette model, which has a phase transition from a Z_2 topologically ordered to a spin-polarized state. By mapping the Wen-plaquette model onto a one-dimensional quantum Ising model, we calculate the expectation value of the plaquette operator F_i during a slowly quenching process from a topologically ordered state. A logarithmic scaling law of quench dynamics near the quantum phase transition is found, which is analogous to the well-known static critical behavior of the specific heat in the one-dimensional quantum Ising model.

I. INTRODUCTION

Ultracold atoms provide an ideal platform for experimental studies of the time evolution of quantum systems, and make it desirable for related theoretical explorations on dynamics of quantum phase transitions in various models. These explorations mainly focus on nonequilibrium dynamics in quantum systems which undergo a quantum phase transition when a system parameter is varied (*quantum quench*)[1]. These experimental and theoretical studies can potentially help to pave the way for future technologies and provide a deeper understanding of quantum many-body physics, particularly the universal scaling behavior in quench dynamics.

Recently, a new type of phase transition, the so-called topological quantum phase transition (TQPT) has attracted considerable research attention[2–13]. TQPT is a kind of phase transition between two quantum states with the *same* symmetry. It is fundamentally different from the usual symmetry-breaking phase transition, and involves a new type of order — *topological order*, as introduced by Wen[14]. In such an ordered state, there is no local order parameter, and the state is robust against arbitrary local perturbations. On this basis, quantum systems with topological order have been proposed to build robust quantum memories[6] and topological quantum computer (TQC)[15, 16]. In Refs. [15, 16], it was shown that the pure state of topological order can be obtained via an adiabatical and continuous evolution process from a non-topologically ordered state and further be used as the initial state for TQC. Nevertheless, the detailed dynamics of such a quench process, particularly the universal scaling behavior near TQPT, had not been studied yet.

In the last decade, several exactly solvable spin models with topological order were found, such as the toric-code model[6], the Wen-plaquette model[17] and the Kitaev model on a hexagonal lattice[18]. These spin models provide a framework to study the TQPT and its quench dynamics. Thus, in recent years, some research groups have studied the quench dynamics of TQPT in the Kitaev model (e.g. Mondal *et al.* [19]) or the toric-code model (e.g. Tsomokos *et al.* [20]). Mondal *et al.* found a relationship between the quench rate and the defect density in the one-dimensional (1D) and two-dimensional (2D) Kitaev model in the limit of slow quench rate and generalized the result to the defect density of a d dimensional quantum model. Tsomokos *et al.* investigated how a topologically ordered ground state in the toric-code model reacts to rapid quenches. They tested several cases and showed which kind of quench can preserve or suppress the topological order.

In this work, we study the quench dynamics of TQPT from a topologically ordered state to a non-topologically ordered one in the Wen-plaquette model. To characterize the phase transition, we calculate the expectation value of plaquette operator F_i during the quenching process, which is related to the number of quasiparticles in the topologically ordered state. Our results provide helpful information about the whole quenching process.

The remaining of this paper is organized as follows. Section II describes an exact mapping from the 2D transverse Wen-plaquette model onto the 1D Ising chain. In Sec. III, we study the TQPT of the 2D transverse Wen-plaquette model and give some results about its order parameters. In Sec. IV, we give the solutions to the dynamics of TQPT in the transverse Wen-plaquette model. A brief discussion is given in Sec. V.

II. MAPPING THE TRANSVERSE WEN-PLAQUETTE ONTO ISING MODEL

We start with the Hamiltonian of the Wen-plaquette model on a square lattice with periodic boundary conditions in both directions:

$$H_W = -g\sum_i F_i, \quad F_i = \tau_i^y \tau_{i+\hat{x}}^x \tau_{i+\hat{x}+\hat{y}}^y \tau_{i+\hat{y}}^x, \qquad (1)$$

where τ_i^x and τ_i^y are Pauli operators on site i, $\hat{x}$ and $\hat{y}$ are the unit vectors in x-axis and y-axis, respectively (see Fig. 1). Because of the commutativity of H and F_i, the energy eigenstates can be labeled by the eigenstates of F_i. We can easily find $F_i^2 = 1$, so the eigenvalues of F_i are

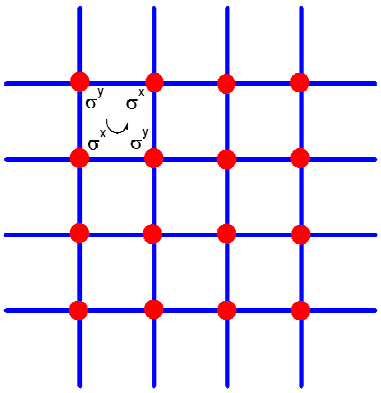

FIG. 1: (Color online) The lattice where Wen-plaquette model is located. A plaquette is defined by $F_i = \tau_i^y \tau_{i+\hat{x}}^x \tau_{i+\hat{x}+\hat{y}}^y \tau_{i+\hat{y}}^x$.

$F_i = 1$ and $F_i = -1$, which gives the exact ground state energy. In the case of $g > 0$, the ground state is $F_i = 1$ for every plaquette, and the elementary excitation is $F_i = -1$ on one plaquette (denoted by i) with an energy gap $E_g - E_0 = 2g$. On an even-by-even lattice, there are two types of plaquettes — the even plaquettes and the odd plaquettes, respectively. As a result, one may define two kinds of bosonic quasiparticles: Z_2 charge and Z_2 vortex (see detailed calculations in Ref. [17] or Ref. [2]). A Z_2 charge is defined by $F_i = -1$ on an even sub-plaquette while a Z_2 vortex defined by $F_i = -1$ on an odd one. Thus a fermion can be regarded as the bound state of a Z_2 charge and a Z_2 vortex.

Now we consider the Wen-plaquette model in a transverse field, which is defined by:

$$H'_W = -g \sum_i F_i - J \sum_i \tau_i^x. \tag{2}$$

This model on a square lattice can be mapped onto the 1D quantum Ising model with the Hamiltonian [11]

$$H_I = -J \sum_{n=1}^{N} (g_I \sigma_n^x + \sigma_n^z \sigma_n^z), \tag{3}$$

where σ_n^x and σ_n^z are Pauli operators.

To derive the mapping, one can calculate the commutation relations (see detailed calculations in Appendix):

$$\begin{aligned} &[F_i, \tau_j^x] = 2F_i \tau_j^x (\delta_{i,j-\hat{x}} + \delta_{i,j-\hat{y}}), \\ &[F_i, F_j] = 0, \\ &[\tau_i^x, \tau_j^x] = 0. \end{aligned} \tag{4}$$

These relations correspond to those in Ising model:

$$\begin{aligned} &[\sigma_i^x, \sigma_j^z \sigma_{j+1}^z] = 2\sigma_i^x \sigma_j^z \sigma_{j+1}^z (\delta_{i,j} + \delta_{i,j+1}), \\ &[\sigma_i^x, \sigma_j^x] = 0, \\ &[\sigma_i^z \sigma_{i+1}^z, \sigma_j^z \sigma_{j+1}^z] = 0. \end{aligned} \tag{5}$$

Then we obtain the mapping

$$F_i \leftrightarrow \sigma_i^x, \quad \tau_i^x \leftrightarrow \sigma_i^z \sigma_{i+1}^z. \tag{6}$$

Accordingly, the Hamiltonian (2) can be mapped onto the 1D quantum Ising model:

$$H'_W \to -\sum_\alpha \sum_i (g\sigma_{\alpha i}^x + J\sigma_{\alpha i}^z \sigma_{\alpha i+1}^z), \tag{7}$$

where the subscript α implies there is one or more Ising chains. The number of Ising chains is determined by the size of the square lattice for the Wen-plaquette model (see Ref.[11]). Since the Ising chains decouple from each other, we can consider only one Ising chain without loss of generality, and reduce the Hamiltonian (7) to

$$H'_W = -J \sum_i (g_I \sigma_i^x + \sigma_i^z \sigma_{i+1}^z), \quad g_I = \frac{g}{J}. \tag{8}$$

Then we may explore the quantum properties of the original Wen-plaquette model by studying the corresponding 1D Ising model.

III. STRING ORDER PARAMETERS IN THE WEN-PLAQUETTE MODEL

For the 1D transverse Ising model (3), there are two phases: in the limit of $g_I \gg 1$, the ground state is a paramagnet with all spins polarized along x-axis, $\langle \sigma_i^x \rangle \to 1$; in the limit of $g_I \ll 1$, there are two degenerate ferromagnetic ground states with all spins along positive or negative z-axis and $\langle \sigma_i^x \rangle \to 0$. Consequently, in Hamiltonian (8), there is a quantum critical point at[21]

$$g_I = \frac{g}{J} = 1 \tag{9}$$

that divides the two phases. Accordingly, the original transverse Wen-plaquette model also has two phases separated by this quantum critical point — in the region of $g_I > 1$, the system is a topologically ordered state; in the region of $g_I < 1$, it is a spin-polarized state.

Noting that the local order parameters cannot be used to learn the nature of TQPT any more, we introduce two non-local order parameters ψ_1 and ψ_2 as string order parameters (SOP's) in the transverse Wen-plaquette model. They are defined by the expectations of string operators $\prod_i F_i$ and $\prod_i \tau_i^x$ with i the site index along a string in the diagonal direction[11], i.e. $\psi_1 \equiv \langle \prod_i F_i \rangle$ and $\psi_2 \equiv \langle \prod_i \tau_i^x \rangle$, respectively.

We then calculate these two SOP's by using the mapping of Eq.(6). For ψ_2, one has

$$\psi_2 = \left\langle \prod_i \tau_i^x \right\rangle = \left\langle \sigma_1^z \sigma_2^z \sigma_2^z \sigma_3^z \cdots \sigma_{n-1}^z \sigma_n^z \right\rangle = \left\langle \sigma_1^z \sigma_n^z \right\rangle, \tag{10}$$

which is the correlation of two spins in the Ising chain of length n. By the Jordan-Wigner transformation

$$\sigma_n^x = 1 - 2c_n^\dagger c_n, \quad \sigma_n^z = -(c_n + c_n^\dagger)\nu, \tag{11}$$

where

$$\nu \equiv \prod_{m<n}(1-2c_m^\dagger c_m) = \prod_{m<n}(c_m c_m^\dagger - c_m^\dagger c_m) = \prod_{m<n} A_m B_m, \tag{12}$$

and $A_m = c_m^\dagger + c_m$, $B_m = c_m^\dagger - c_m$, $c_m^\dagger$ and c_m are the creation and annihilation operators for fermions, we obtain

$$\begin{aligned}\psi_2 = \langle \sigma_1^z \sigma_n^z \rangle &= \left\langle (c_1 + c_1^\dagger)\nu(c_n + c_n^\dagger) \right\rangle \\ &= \langle B_1 A_2 B_2 \cdots B_{n-1} A_n \rangle \,. \end{aligned} \tag{13}$$

Following the Wick's theorem, we can transform Eq.(13) into a Toeplitz determinant as[22]

$$\begin{vmatrix} G_{12} & G_{13} & \cdots & G_{1n} \\ G_{22} & G_{23} & \cdots & G_{2n} \\ \vdots & \vdots & \ddots & \vdots \\ G_{n-1,2} & G_{n-1,3} & \cdots & G_{n-1,n} \end{vmatrix}, \tag{14}$$

where

$$G_{ij} = -\frac{1}{2\pi}\int_{-\pi}^{\pi} \mathrm{d}k \frac{g_I - \cos k - i \sin k}{\sqrt{(g_I - \cos k)^2 + \sin^2 k}} e^{ik(i-j)}. \tag{15}$$

In the thermodynamic limit $N \to \infty$, we have (see Ref. [23] or Ref. [24])

$$\psi_2 \sim \begin{cases} (1-g_I^2)^{1/4} & \text{when } g_I < 1 \\ 0 & \text{when } g_I \geq 1 \end{cases}. \tag{16}$$

The exponent 1/4 here agrees with the critical exponent $2\beta/\nu = 1/4$ (see Ref.[21]).

By the same method we can obtain the result of ψ_1,

$$\psi_1 = \left\langle \prod_i F_i \right\rangle = \left\langle \prod_i \sigma_i^x \right\rangle. \tag{17}$$

In addition, we can take advantage of the duality of 1D Ising model (see Ref. [22]) :

$$s_i^x = \sigma_i^z \sigma_{i+1}^z \quad \text{and} \quad s_i^z = \prod_{k<i} \sigma_k^x. \tag{18}$$

Thus, Eq. (17) turns into $\psi_1 = m$, where $m \equiv \langle \sigma_i^z \rangle$ is the spontaneous magnetization. We find that when $N \to \infty$, the spin correlation (10) is the square of m. Consequently, from Eq. (16), we have

$$\psi_1 \sim \begin{cases} 0 & \text{when } g_I \leq 1 \\ (1-g_I^{-2})^{1/8} & \text{when } g_I > 1 \end{cases}. \tag{19}$$

From the calculations above, one may notice that the non-local SOPs in a 2D transverse Wen-plaquette model are transformed to local order parameters in the dual 1D Ising model.

IV. QUENCH DYNAMICS OF TQPT

In this section we study the dynamics of TQPT in the transverse Wen-plaquette model. The Kibble-Zurek mechanism (KZM)[25, 26] is a general theory to explore the dynamics of second order phase transitions including the quantum case. According to KZM, during a quench-induced phase transition, the system undergoes three stages of evolution: adiabatic–pulse–adiabatic. It predicts that the density of topological defects, which are generated by the pulse evolution, is a function of quench time.

We can solve the dynamic problems in the Wen-plaquette model by taking a sequence of transformations as in Ref. [27]. First, through the Jordan-Wigner transformation (11), the spin operators $\sigma_i^{x,z}$ are represented by fermionic operators c_n. Second, c_n are Fourier transformed into the momentum space:

$$c_n = \frac{e^{-i\pi/4}}{\sqrt{N}} \sum_k c_k e^{ikn}. \tag{20}$$

Third, after Bogoliubov transformation, one have

$$c_k = u_k \eta_k + v_{-k}^* \eta_{-k}^\dagger, \tag{21}$$

where η_k and $\eta_k^\dagger$ are fermionic operators. For dynamic problems, (21) becomes

$$c_k(t) = u_k(t)\widetilde{\eta}_k + v_{-k}^*(t)\widetilde{\eta}_{-k}^\dagger. \tag{22}$$

Now, a dynamic solution can be written in the form of Bogoliubov modes ($u_k(t)$, $v_k(t)$) after this whole transformation procedure.

By this method, the dynamics of the quantum Ising model can be expressed as the time evolution of the Bogoliubov modes via the so-called Bogoliubov-de Gennes dynamic equations (see Ref. [27]):

$$\begin{cases} i\hbar \mathrm{d}u_k/\mathrm{d}t = +2(g_I(t) - \cos k)u_k + 2\sin k v_k \\ i\hbar \mathrm{d}v_k/\mathrm{d}t = -2(g_I(t) - \cos k)v_k + 2\sin k u_k \end{cases}. \tag{23}$$

Consider a linear quench, i.e.

$$g_I(t<0) = -\frac{t}{\tau_Q}, \tag{24}$$

where t varies from $-\infty$ to 0 and the quench time τ_Q characterizes the quench rate (defined by $1/\tau_Q$). Equations (23) can be transformed into the form of Landau-Zener (LZ) model[28] (the connection between the KZM and the LZ model can be found in Ref. [29, 30]) :

$$\begin{cases} i\hbar \mathrm{d}u_k/\mathrm{d}\tau = -\frac{1}{2}(\tau\Delta_k)u_k + \frac{1}{2}v_k \\ i\hbar \mathrm{d}v_k/\mathrm{d}\tau = +\frac{1}{2}(\tau\Delta_k)v_k + \frac{1}{2}u_k \end{cases}, \tag{25}$$

where

$$\tau = 4\tau_Q \sin k(\frac{t}{\tau_Q} + \cos k),$$

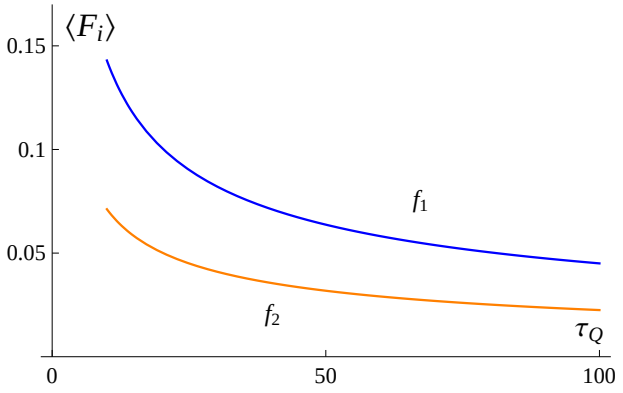

FIG. 2: (Color online) The expectation value of F_i at $t = 0$ varying with the quench time τ_Q, where $f_1 = 1 - \frac{1}{\pi}\int_{-\pi}^{\pi} \mathrm{d}k(\frac{1+\cos k}{2} - e^{-2\pi\tau_Q \sin^2 k})$ and the approximative result $f_2 = \frac{1}{\pi\sqrt{2\tau_Q}}$.

and

$$\Delta_k^{-1} = 4\tau_Q \sin^2 k.$$

From equations (25), we derive a second order differential equation for v_k:

$$\frac{\mathrm{d}^2 v_k}{\mathrm{d}\tau^2} + (\frac{1}{4}\tau^2\Delta_k^2 + \frac{i\Delta_k}{2} + \frac{1}{4})v_k = 0. \tag{26}$$

After the substitutions

$$s = \frac{1}{4i\Delta_k} \quad \text{and} \quad z = \sqrt{\Delta_k}\tau e^{i\pi/4}, \tag{27}$$

we have

$$\frac{\mathrm{d}^2 v_k(z)}{\mathrm{d}z^2} + (s + \frac{1}{2} - \frac{1}{4}z^2)v_k(z) = 0. \tag{28}$$

This kind of differential equation has a general solution

$$\begin{aligned} v_k(\tau) &= -[aD_{-s-1}(-iz) + bD_{-s-1}(iz)], \\ u_k(\tau) &= (-\Delta_k\tau + 2i\tfrac{\partial}{\partial\tau})v_k(\tau), \end{aligned} \tag{29}$$

where $D_m(x)$ is the so-called parabolic cylinder function (PCF) or Weber-Hermite function[31].

According to the boundary conditions and the characters of the PCF, one may derive approximate solutions of Eqs. (28) at the end of the linear quench (for $t = 0$) (See Ref. [27]):

$$\begin{aligned} &|u_k|^2 = \tfrac{1-\cos k}{2} + e^{-2\pi\tau_Q \sin^2 k}, \\ &|v_k|^2 = 1 - |u_k|^2, \\ &u_k v_k^* = \tfrac{1}{2}\sin k + \mathrm{sgn}(k)e^{-\pi\tau_Q \sin^2 k}\sqrt{1 - e^{-\pi\tau_Q \sin^2 k}}e^{i\varphi_k}, \end{aligned} \tag{30}$$

with the condition $\tau_Q \gg 1$.

Now we calculate the dynamic solutions in the Wen-plaquette model via the same transformation procedure plus the mapping (6). We shall also consider Eq. (24). The quenching process corresponds to tuning the strength of the transverse field from zero to a very large value compared with the coupling constant g. The phase transition is thus from a topologically ordered state to a spin-polarized state during the time-evolution from $t = -\infty$ to $t = 0$.

First, we calculate the expectation value of F_i after the quenching process. From Jordan-Wigner transformation, $\sigma_n^x = 1 - 2c_n^\dagger c_n$, we have the mapping:

$$\langle F_i\rangle \to \langle\sigma_n^x\rangle = \left\langle\left(1 - 2c_n^\dagger c_n\right)\right\rangle.$$

Through the Fourier transformation, we express $c_m^\dagger c_n$ in momentum space

$$c_m^\dagger c_n = \frac{1}{2\pi}\int_{-\pi}^{\pi}\mathrm{d}k\int_{-\pi}^{\pi}\mathrm{d}k' c_k^\dagger c_{k'} e^{i(k'n-km)}. \tag{31}$$

After the Bogoliubov transformation (21), we obtain[32]

$$\begin{aligned} \langle c_m^\dagger c_n\rangle &= \frac{1}{2\pi}\int_{-\pi}^{\pi}\mathrm{d}k\int_{-\pi}^{\pi}\mathrm{d}k' e^{i(k'n-km)} v_{-k}v_{-k}^*\delta_{k,k'} \\ &= \frac{1}{2\pi}\int_{-\pi}^{\pi}\mathrm{d}k|v_k|^2 e^{ik(n-m)}. \end{aligned} \tag{32}$$

From the solutions (30), we derive

$$\begin{aligned} \langle F_i\rangle \to \langle\sigma_n^x\rangle = 1 - 2\cdot\frac{1}{2\pi}\int_{-\pi}^{\pi}\mathrm{d}k(\frac{1+\cos k}{2} \\ - e^{-2\pi\tau_Q \sin^2 k}) \overset{\tau_Q\gg 1}{\simeq} \frac{1}{\pi\sqrt{2\tau_Q}}. \end{aligned} \tag{33}$$

We can see that the original topological ground state with $\langle F_i\rangle = 1$ (see the discussion below Eq. (1)) will finally evolve into the trivial spin-polarized state with $\langle F_i\rangle \to \langle\sigma_n^x\rangle \to 0$ for an infinitely slow quench. Figure 2 shows how the expectation value of F_i at the end of quenching process ($t = 0$) varies with the quench rate.

We can obtain the numbers of Z_2 charges and Z_2 vortices by defining

$$\mathcal{N}_c \equiv \frac{1}{2}\sum_{i\in\text{even}}(1 - F_i) = \sum_{i\in\text{even}} c_i^\dagger c_i \tag{34}$$

and

$$\mathcal{N}_v \equiv \frac{1}{2}\sum_{i\in\text{odd}}(1 - F_i) = \sum_{i\in\text{odd}} c_i^\dagger c_i,$$

respectively. Before the quench, the system is in a topological ground state. There is no quasiparticles ($N_c \equiv \langle\mathcal{N}_c\rangle = 0$, $N_v \equiv \langle\mathcal{N}_v\rangle = 0$), so we have $F_i = 1$ for all plaquettes. At the end of the quench, we can also calculate the density of plaquettes $F_i = -1$[33] by

$$\begin{aligned} n = \frac{1}{2N}\langle\sum_i(1 - F_i)\rangle = \frac{1}{2\pi}\int_{-\pi}^{\pi}\mathrm{d}k(\frac{1+\cos k}{2} \\ - e^{-2\pi\tau_Q \sin^2 k}) \overset{\tau_Q\gg 1}{\simeq} \frac{1}{2} - \frac{1}{2\pi\sqrt{2\tau_Q}}. \end{aligned} \tag{35}$$

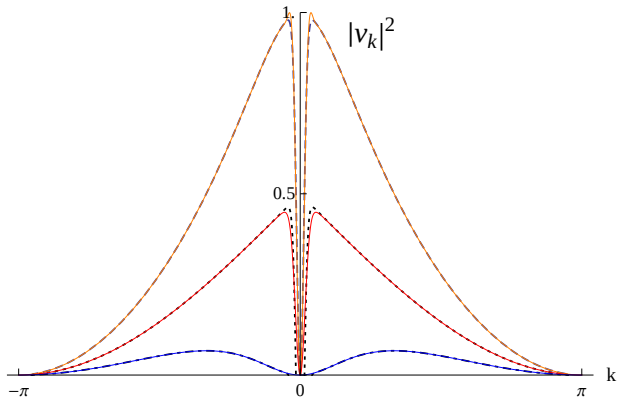

FIG. 3: (Color online) The colored curves represent $|v_k(\tau)|^2$ in the original form of the PCF varying with momenta k from $-\pi$ to π, where the orange one is at $t = -0.5\tau_Q$, the red at $t = -\tau_Q$, the blue at $t = -2\tau_Q$ with $\tau_Q = 50$ in all the three cases. The dashed, dotted and dot-dashed curves, respectively, represent the approximate function for $|v_k(\tau)|^2$ with corresponding parameters, with the negative parts under the x-axis being cut off. They match with the colored curves very well.

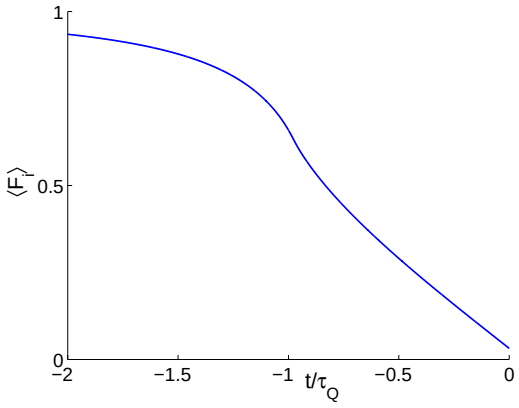

FIG. 4: (Color online) The expectation value of F_i during the quenching process varying from $t = -2\tau_Q$ to $t = 0$ with $\tau_Q = 50$.

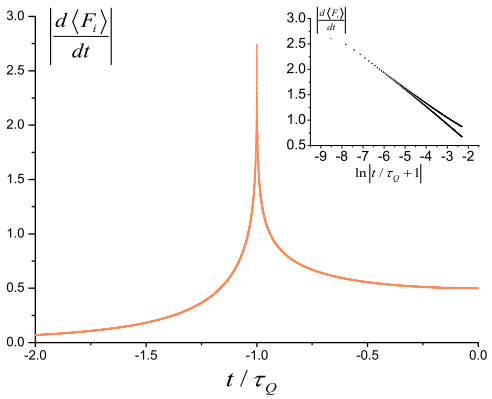

FIG. 5: (Color online) The absolute value of the slope ($|\frac{\mathrm{d}\langle F_i\rangle}{\mathrm{d}t}|$) corresponding to the curve above. The small graph shows $|\frac{\mathrm{d}\langle F_i\rangle}{\mathrm{d}t}| \sim \ln|t/\tau_Q + 1|$ from both sides approaching the critical point $t = -\tau_Q$.

It is obvious that when $\tau_Q \to \infty$, half of the plaquettes will be turned into $F_i = -1$, which implies $\langle F_i\rangle \to 0$.

However, this result cannot give us any information about the quenching process or the critical behaviors. In order to obtain such information, we find that, for $\tau_Q \gg 1$, the expression

$$|v_k(t)|^2 = \frac{1}{2}(1+\frac{\cos k + t/\tau_Q}{\sqrt{1+2t/\tau\cos k+(t/\tau_Q)^2}})-e^{-2\pi\tau_Q \sin^2 k} \tag{36}$$

is a time-dependent approximate function for the general solution $|v_k(\tau)|^2$ in Eq. (29), if we cut off the negative part of the curve (see Fig. 3).

By using this approximate function, we calculate the value $\langle F_i\rangle$ during the quenching process as a function of the time t near the quantum critical point. The result is shown in Fig. 4 and Fig. 5.

Further calculations show that the derivative of the expectation-value $\langle F_i\rangle$ diverges at point $t = t_c = -\tau_Q$ as $\frac{\mathrm{d}\langle F_i\rangle}{\mathrm{d}t} \to -\infty$, which characterizes the critical point. In particular, we obtain a logarithmic scaling law of quench dynamics near the quantum phase transition

$$\frac{\mathrm{d}\langle F_i\rangle}{\mathrm{d}t} \sim \ln|t - t_c|. \tag{37}$$

Such a dynamics is analogous to the static scaling behavior of the specific heat near the critical point for the 1D quantum Ising model.

The physical picture can be described as follows. At beginning, the external field is weak and can be treated as a perturbation, which creates vortices or charges and drives them to move around and annihilate each other. As a result, the density of quasiparticles remains small. As the strength of the field continuous to grow, the density of plaquettes $F_i = -1$ increases rapidly near the point $g_I = 1$ (that is $t = -\tau_Q$). The rate of density-changing diverges with a logarithmic scaling law. Finally, at the end of the quench, the field becomes so strong that the vortices and charges are all confined and cannot be treated as quasiparticles. If the quenching process is infinitely slow, half of the plaquttes overturns.

In addition we shall notice that only the linear quench is considered here. Indeed, for other cases, our method is not reliable. Inspired by other papers on quantum quench in the toric-code model (e.g. Rahmani *et al.* [34], where a sudden quench is studied), we could study the quench problem more generally through the time evolution of the entanglement entropy in the Wen-plaquette model. Yet,

we did not consider this in this work.

V. CONCLUSION

In summary, we study the dynamics of TQPT caused by a linear quench in the transverse Wen-plaquette model. We first show how to derive the mapping from the 2D Wen-plaquette onto the 1D Ising model by comparing their commutation relations. Based on this mapping, we point out the quantum critical point in the transverse Wen-plaquette model and calculate its non-local order parameters. We then calculate the expectation value of F_i at the end of the quench, and further show how this value varies during the whole process. In particular, we find a logarithmic scaling law of quenching process near the TQPT.

Finally we address the relationship between the Wen-plaquette model and the Kitaev model on a 2D hexagonal lattice. The Abelian topological ground states of the Kitaev model on a 2D hexagonal lattice are also the Z_2 topologically ordered ones just like those of the Wen-plaquette model. However, one cannot map the Kitaev model on a 2D hexagonal lattice onto a 1D Ising chain (except for the case of the anisotropic limit) as what we have done for the 2D transverse Wen-plaquette model. As a result, the quench dynamics of TQPT in Wen-plaquette model is different from that in the Kitaev model.

The authors acknowledge that this research is supported by NFSC Grant No. 10874017, 10975127, National Basic Research Program of China (973 Program) under the grant No. 2011CB921803, 2011CB92180 and 2011CB921304, the Anhui Provincial Natural Science Foundation under Grant No. 090416224, and the Chinese Academy of Sciences.

Appendix

In this part, we give detailed calculations about commutation relations (4), which is related to the consistency between Wen-plaquette model and Ising model.

The key point is to calculate $[F_i, F_j]$,

$$\begin{aligned}
&[F_i, F_j] \\
&= [\tau_i^x \tau_{i+\hat{x}}^y \tau_{i+\hat{y}+\hat{x}}^x \tau_{i+\hat{y}}^y, \tau_j^x \tau_{j+\hat{x}}^y \tau_{j+\hat{y}+\hat{x}}^x \tau_{j+\hat{y}}^y] \\
&= [\tau_i^x, \tau_j^x \tau_{j+\hat{x}}^y \tau_{j+\hat{y}+\hat{x}}^x \tau_{j+\hat{y}}^y] \tau_{i+\hat{x}}^y \tau_{i+\hat{y}+\hat{x}}^x \tau_{i+\hat{y}}^y + \tau_i^x \\
&[\tau_{i+\hat{x}}^y, \tau_j^x \tau_{j+\hat{x}}^y \tau_{j+\hat{y}+\hat{x}}^x \tau_{j+\hat{y}}^y] \tau_{i+\hat{y}+\hat{x}}^x \tau_{i+\hat{y}}^y + \tau_i^x \tau_{i+\hat{x}}^y \\
&[\tau_{i+\hat{y}+\hat{x}}^x, \tau_j^x \tau_{j+\hat{x}}^y \tau_{j+\hat{y}+\hat{x}}^x \tau_{j+\hat{y}}^y] \tau_{i+\hat{y}}^y + \tau_i^x \tau_{i+\hat{x}}^y \tau_{i+\hat{y}+\hat{x}}^x \\
&[\tau_{i+\hat{y}}^y, \tau_j^x \tau_{j+\hat{x}}^y \tau_{j+\hat{y}+\hat{x}}^x \tau_{j+\hat{y}}^y]. \qquad (38)
\end{aligned}$$

According to the commutation relations of Pauli operators,

$$\begin{aligned}
&[\tau_i^x, \tau_j^x \tau_{j+\hat{x}}^y \tau_{j+\hat{y}+\hat{x}}^x \tau_{j+\hat{y}}^y] \\
&= [\tau_i^x, \tau_j^x] \tau_{j+\hat{x}}^y \tau_{j+\hat{y}+\hat{x}}^x \tau_{j+\hat{y}}^y + \tau_j^x [\tau_i^x, \tau_{j+\hat{x}}^y] \tau_{j+\hat{y}+\hat{x}}^x \tau_{j+\hat{y}}^y \\
&+ \tau_j^x \tau_{j+\hat{x}}^y [\tau_i^x, \tau_{j+\hat{y}+\hat{x}}^x] \tau_{j+\hat{y}}^y + \tau_j^x \tau_{j+\hat{x}}^y \tau_{j+\hat{y}+\hat{x}}^x [\tau_i^x, \tau_{j+\hat{y}}^y] \\
&= 2i\delta_{i,j+\hat{x}} \tau_j^x \tau_i^z \tau_{j+\hat{y}+\hat{x}}^x \tau_{j+\hat{y}}^y + 2i\delta_{i,j+\hat{y}} \tau_j^x \tau_{j+\hat{x}}^y \tau_{j+\hat{y}+\hat{x}}^x \tau_i^z; \qquad (39)
\end{aligned}$$

$$\begin{aligned}
&[\tau_{i+\hat{x}}^y, \tau_j^x \tau_{j+\hat{x}}^y \tau_{j+\hat{y}+\hat{x}}^x \tau_{j+\hat{y}}^y] \\
&= [\tau_{i+\hat{x}}^y, \tau_j^x] \tau_{j+\hat{x}}^y \tau_{j+\hat{y}+\hat{x}}^x \tau_{j+\hat{y}}^y + \tau_j^x [\tau_{i+\hat{x}}^y, \tau_{j+\hat{x}}^y] \tau_{j+\hat{y}+\hat{x}}^x \tau_{j+\hat{y}}^y \\
&+ \tau_j^x \tau_{j+\hat{x}}^y [\tau_{i+\hat{x}}^y, \tau_{j+\hat{y}+\hat{x}}^x] \tau_{j+\hat{y}}^y + \tau_j^x \tau_{j+\hat{x}}^y \tau_{j+\hat{y}+\hat{x}}^x [\tau_{i+\hat{x}}^y, \tau_{j+\hat{y}}^y] \\
&= -2i\delta_{i+\hat{x},j} \tau_j^z \tau_{j+\hat{x}}^y \tau_{j+\hat{y}+\hat{x}}^x \tau_{j+\hat{y}}^y - 2i\delta_{i,j+\hat{y}} \tau_j^x \tau_{j+\hat{x}}^y \tau_{j+\hat{y}+\hat{x}}^z \\
&\tau_{j+\hat{y}}^y; \qquad (40)
\end{aligned}$$

$$\begin{aligned}
&[\tau_{i+\hat{x}+\hat{x}}^x, \tau_j^x \tau_{j+\hat{x}}^y \tau_{j+\hat{y}+\hat{x}}^x \tau_{j+\hat{y}}^y] \\
&= [\tau_{i+\hat{x}+\hat{x}}^x, \tau_j^x] \tau_{j+\hat{x}}^y \tau_{j+\hat{y}+\hat{x}}^x \tau_{j+\hat{y}}^y + \tau_j^x [\tau_{i+\hat{x}+\hat{x}}^x, \tau_{j+\hat{x}}^y] \tau_{j+\hat{y}+\hat{x}}^x \\
&\tau_{j+\hat{y}}^y + \tau_j^x \tau_{j+\hat{x}}^y [\tau_{i+\hat{x}+\hat{x}}^x, \tau_{j+\hat{y}+\hat{x}}^x] \tau_{j+\hat{y}}^y + \tau_j^x \tau_{j+\hat{x}}^y \tau_{j+\hat{y}+\hat{x}}^x \\
&[\tau_{i+\hat{x}+\hat{x}}^x, \tau_{j+\hat{y}}^y] \\
&= 2i\delta_{i+\hat{y},j} \tau_j^x \tau_{j+\hat{x}}^z \tau_{j+\hat{y}+\hat{x}}^x \tau_{j+\hat{y}}^y + 2i\delta_{i+\hat{x},j} \tau_j^x \tau_{j+\hat{x}}^y \tau_{j+\hat{y}+\hat{x}}^x \\
&\tau_{j+\hat{y}}^z; \qquad (41)
\end{aligned}$$

$$\begin{aligned}
&[\tau_{i+\hat{y}}^y, \tau_j^x \tau_{j+\hat{x}}^y \tau_{j+\hat{y}+\hat{x}}^x \tau_{j+\hat{y}}^y] \\
&= [\tau_{i+\hat{y}}^y, \tau_j^x] \tau_{j+\hat{x}}^y \tau_{j+\hat{y}+\hat{x}}^x \tau_{j+\hat{y}}^y + \tau_j^x [\tau_{i+\hat{y}}^y, \tau_{j+\hat{x}}^y] \tau_{j+\hat{y}+\hat{x}}^x \tau_{j+\hat{y}}^y \\
&+ \tau_j^x \tau_{j+\hat{x}}^y [\tau_{i+\hat{y}}^y, \tau_{j+\hat{y}+\hat{x}}^x] \tau_{j+\hat{y}}^y + \tau_j^x \tau_{j+\hat{x}}^y \tau_{j+\hat{y}+\hat{x}}^x [\tau_{i+\hat{y}}^y, \tau_{j+\hat{y}}^y] \\
&= -2i\delta_{i+\hat{y},j} \tau_j^z \tau_{j+\hat{x}}^y \tau_{j+\hat{y}+\hat{x}}^x \tau_{j+\hat{y}}^y - 2i\delta_{i,j+\hat{x}} \tau_j^x \tau_{j+\hat{x}}^y \tau_{j+\hat{y}+\hat{x}}^z \\
&\tau_{j+\hat{y}}^y, \qquad (42)
\end{aligned}$$

we can calculate (38) in following four cases:

1. when $i = j + \hat{x}$,

$$\begin{aligned}
&[F_i, F_j] \\
&= 2i\tau_j^x \tau_{j+\hat{x}}^z \tau_{j+\hat{y}+\hat{x}}^x \tau_{j+\hat{y}}^y \tau_{i+\hat{x}}^y \tau_{i+\hat{y}+\hat{x}}^x \tau_{i+\hat{y}}^y - 2i\tau_i^x \tau_{i+\hat{x}}^y \tau_{i+\hat{y}+\hat{x}}^x \\
&\tau_j^x \tau_{j+\hat{x}}^y \tau_{j+\hat{y}+\hat{x}}^z \tau_{j+\hat{y}}^y \\
&= -2\tau_j^x \tau_{j+\hat{x}}^z \tau_{j+\hat{y}+\hat{x}}^z \tau_{j+\hat{y}}^y \tau_{i+\hat{x}}^y \tau_{i+\hat{y}+\hat{x}}^x + 2\tau_{i+\hat{x}}^y \tau_{i+\hat{y}+\hat{x}}^x \tau_j^x \tau_{j+\hat{x}}^z \\
&\tau_{j+\hat{y}+\hat{x}}^z \tau_{j+\hat{y}}^y \\
&= 0; \qquad (43)
\end{aligned}$$

2. when $i = j + \hat{y}$,

$$\begin{aligned}
&[F_i, F_j] \\
&= 2i\tau_j^x \tau_{j+\hat{x}}^y \tau_{j+\hat{y}+\hat{x}}^x \tau_{j+\hat{y}}^z \tau_{i+\hat{x}}^y \tau_{i+\hat{y}+\hat{x}}^x \tau_{i+\hat{y}}^y - 2i\tau_i^x \tau_j^x \tau_{j+\hat{x}}^y \\
&\tau_{j+\hat{y}+\hat{x}}^z \tau_{j+\hat{y}}^y \tau_{i+\hat{y}+\hat{x}}^x \tau_{i+\hat{y}}^y \\
&= -2\tau_j^x \tau_{j+\hat{x}}^y \tau_{j+\hat{y}+\hat{x}}^z \tau_{j+\hat{y}}^z \tau_{i+\hat{y}+\hat{x}}^x \tau_{i+\hat{y}}^y + 2\tau_{j+\hat{y}}^z \tau_j^x \tau_{j+\hat{x}}^y \tau_{j+\hat{y}+\hat{x}}^z \\
&\tau_{i+\hat{y}+\hat{x}}^x \tau_{i+\hat{y}}^y \\
&= 0; \qquad (44)
\end{aligned}$$

3. when $i+\hat{x}=j$

$$
\begin{aligned}
&[F_i,F_j]\\
&=-2i\tau_i^x\tau_j^z\tau_{j+\hat{x}}^y\tau_{j+\hat{y}+\hat{x}}^x\tau_{j+\hat{y}}^y\tau_{i+\hat{y}+\hat{x}}^x\tau_{i+\hat{y}}^y+2i\tau_i^x\tau_{i+\hat{x}}^y\tau_j^x\tau_{j+\hat{x}}^y\\
&\tau_{j+\hat{y}+\hat{x}}^x\tau_{i+\hat{y}}^z\tau_{i+\hat{y}}^y\\
&=-2\tau_i^x\tau_j^z\tau_{j+\hat{x}}^y\tau_{j+\hat{y}+\hat{x}}^x\tau_{i+\hat{y}+\hat{x}}^z\tau_{i+\hat{y}}^y+2\tau_i^x\tau_{i+\hat{x}}^z\tau_{j+\hat{x}}^y\tau_{j+\hat{y}+\hat{x}}^x\\
&\tau_{j+\hat{y}}^z\tau_{i+\hat{y}}^y\\
&=0;
\end{aligned}
\tag{45}
$$

4. when $i+\hat{y}=j$

$$
\begin{aligned}
&[F_i,F_j]\\
&=2i\tau_i^x\tau_{i+\hat{x}}^y\tau_j^x\tau_{j+\hat{x}}^z\tau_{j+\hat{y}+\hat{x}}^x\tau_{j+\hat{y}}^y\tau_{i+\hat{y}}^y-2i\tau_i^x\tau_{i+\hat{x}}^y\tau_{i+\hat{y}+\hat{x}}^x\tau_j^z\\
&\tau_{j+\hat{x}}^y\tau_{i+\hat{y}+\hat{x}}^x\tau_{i+\hat{y}}^y\\
&=-2\tau_i^x\tau_{i+\hat{x}}^y\tau_j^z\tau_{j+\hat{x}}^z\tau_{j+\hat{y}+\hat{x}}^x\tau_{j+\hat{y}}^y+2\tau_i^x\tau_{i+\hat{x}}^y\tau_{i+\hat{y}+\hat{x}}^z\tau_j^z\tau_{j+\hat{y}+\hat{x}}^x\\
&\tau_{i+\hat{y}}^y\\
&=0.
\end{aligned}
\tag{46}
$$

It is clear that we also have $[F_i,F_j]=0$ in other cases.

Then, we only need to verify $[F_i,\tau_j^x]=2F_i\tau_j^x(\delta_{i,j-\hat{x}}+\delta_{i,j-\hat{y}})$, while others can be easily obtained from the commutation relations of Pauli operators. The verification is shown in the following:

$$
\begin{aligned}
&[F_i,\tau_j^x]\\
&=-2i\delta_{j,i+\hat{x}}\tau_i^x\tau_{i+\hat{x}}^z\tau_{i+\hat{y}+\hat{x}}^x\tau_{i+\hat{y}}^y-2i\delta_{j,i+\hat{y}}\tau_i^x\tau_{i+\hat{x}}^y\tau_{i+\hat{y}+\hat{x}}^x\tau_{i+\hat{y}}^z\\
&=-2\delta_{j,i+\hat{x}}\tau_i^x\tau_{i+\hat{x}}^x\tau_{i+\hat{x}}^y\tau_{i+\hat{y}+\hat{x}}^x\tau_{i+\hat{y}}^y-2\delta_{j,i+\hat{y}}\tau_i^x\tau_{i+\hat{x}}^y\tau_{i+\hat{y}+\hat{x}}^x\\
&\tau_{i+\hat{y}}^x\tau_{i+\hat{y}}^y\\
&=-2\delta_{j,i+\hat{x}}\tau_j^xF_i-2\delta_{j,i+\hat{y}}\tau_j^xF_i\\
&=2F_i\tau_j^x(\delta_{j,i+\hat{x}}+\delta_{j,i+\hat{y}}).
\end{aligned}
\tag{47}
$$

* Corresponding author; Electronic address: spkou@bnu.edu.cn

[1] A. Polkovnikov, K. Sengupta, A. Silva, and M. Vengalattore, arXiv:1007.5331

[2] X.-G. Wen, *Quantum Field Theory of Many-Body Systems* (Oxford University Press, Oxford, 2004).

[3] X. G. Wen, Phys. Rev. B 65, 165113 (2002).

[4] X. G. Wen, Phys. Rev. D **68**, 065003 (2003).

[5] X. G. Wen, Int. J. Mod. Phys. B **4**, 239 (1990).

[6] A. Y. Kitaev, Ann. Phys. (N.Y.) **303**, 2 (2003)

[7] S. Trebst, P. Werner, M. Troyer, K. Shtengel and C. Nayak, Phys. Rev. Lett. **98**, 070602 (2007) .

[8] A. Hamma and D. A. Lidar, Phys. Rev. Lett. **100**, 030502 (2008).

[9] C. Castelnovo and C. Chamon, Phys. Rev. B **76**, 174416 (2007).

[10] X.-Y. Feng, G.-M. Zhang, and T. Xiang, Phys. Rev. Lett. **98**, 087204 (2007).

[11] J. Yu, S.-P. Kou, and X.-G. Wen, Europhys. Lett. **84**, 17004 (2008).

[12] J. Vidal, S. Dusuel, and K.P. Schmidt, Phys. Rev. B **79**, 033109 (2009).

[13] J. Vidal, R. Thomale, K.P. Schmidt, and S. Dusuel, Phys. Rev. B **80**, 081104 (2009).

[14] X.-G. Wen, Phys. Rev. B **40**, 7387 (1989).

[15] S. P. Kou, Phys. Rev. Lett. **102**, 120402 (2009).

[16] S. P. Kou, Phys. Rev. A **80**, 052317 (2009).

[17] X.-G. Wen, Phys. Rev. Lett. **90**, 016803 (2003).

[18] A. Y. Kitaev, Ann. Phys. **321**, 2 (2006).

[19] E. Mondal, D. Sen, and K. Senqupta, Phys. Rev. B **78**, 045101 (2008).

[20] D. I. Tsomokos, A. Hamma, W. Zhang, S. Haas, and R. Fazio, Phys. Rev. A **80**, 060302 (2009).

[21] R. J. Baxter, *Exactly Sovled Models in Statistical Mechanics*, (Academic Press, New York, 1982)

[22] B. K. Chakrabarti, A.Dutta, and P. Sen, *Quantum Ising Phases and Transitions in Transverse Ising Models* (Springer Press, 1996).

[23] B. M. McCoy, Phys. Rev. **173**, 531 (1968).

[24] E. Barouch and B. M. McCoy, Phys. Rev. A **3**, 786 (1971).

[25] T. W. B. Kibble, J. Phys. A **9**, 1387 (1976); Phys. Rep. **67**, 183 (1980).

[26] W. H. Zurek, Nature (London) **317**, 505 (1985); Acta Phys. Pol. B **24**, 1301 (1993); Phys. Rep. **276**, 177 (1996).

[27] J.Dziarmaga, Phys. Rev. Lett. **95**, 245701 (2005); L. Cincio, J. Dziarmaga, M. M. Rams, and W. H. Zurek, Phys. Rev. A **75**, 052321 (2007).

[28] L. Landau and E. M. Lifshitz, *Quantum Mechanics: Non-relativistic Theory*, 2nd Ed. (Pergamon Press, Oxford,1965); C. Zener, Proc. Roy. Soc. Lond. A **137**, 696 (1932).

[29] B. Damski, Phys. Rev. Lett. **95**, 035701 (2005).

[30] B. Damski and W. H. Zurek, Phys. Rev. A **73**, 063405 (2006).

[31] E. T. Whittaker, and G. N. Watson, *A Course of Modern Analysis*, (Cambridge University Press, Cambridge, England, 1958).

[32] The expression (15) is also calculated by this whole procedure.

[33] It should be noticed that Z_2 charges and Z_2 vortices are on longer the elementary excitations or quasipartices of the post-quench system.

[34] A. Rahmani, and C. Chamon, Phys. Rev. B **82**. 134303 (2010).